

Gravity-Assist Maneuvers Augmented by the Lorentz Force

Brett Streetman* and Mason A. Peck†
Cornell University, Ithaca, New York 14853

DOI: 10.2514/1.35676

The effects of Lorentz-augmented orbits on gravity-assist maneuvers are examined. In this study, we consider a spacecraft carrying a net electrostatic charge that performs a hyperbolic flyby of a planet with a nonnegligible magnetosphere. If the charge on the satellite is modulated, the usefulness and effectiveness of the flyby can be extended in several ways with no expenditure of propellant. Both analytical and simulation results are presented for satellites in equatorial orbits within dipole magnetic fields. The spacecraft's exit asymptote from the flyby target's sphere of influence can be changed to an arbitrary direction. The spacecraft can also be captured at the target planet, or the assist maneuver can be timed with more flexibility than a gravity-only flyby.

I. Introduction

GRAVITY-ASSIST, or flyby, maneuvers offer a means to manipulate the energy and momentum of a spacecraft by exploiting interactions with celestial bodies. The principles are well understood and are known to offer a certain capability; specifically, the ΔV that can be achieved is limited by the angle by which the body can deflect the spacecraft's flight path. More generally, ephemerides limit mission architectures. The coupling of launch windows and planetary alignments leads to opportunities and risks at the mission level that shape the way that planetary exploration is done, as has been pointed out many times [1].

Research on Lorentz-augmented orbits (LAOs) has identified physical behaviors that this paper argues can overcome some of these risks and present further opportunities. Specifically, an electrically charged body that passes through a planetary magnetic field experiences a deflection of its flight path in ways that are similar to gravity-assist maneuvers. The primary contribution of this study is the discovery of opportunities to achieve the most effective flyby possible. Here, effectiveness refers to modifying the flight-path angle and allowing for more flexible timing. In turn, this broader class of flyby maneuvers can strengthen outer-planet mission design by reducing the dependence of a mission on specific planetary-alignment geometries and by offering greater overall ΔV .

The Lorentz force experienced by a particle of charge q (coulombs) moving through a magnetic field \mathbf{B} is given by

$$\mathbf{F}_L = q\mathbf{v}_r \times \mathbf{B} \quad (1)$$

where \mathbf{v}_r is the particle velocity with respect to the magnetic field. This force is used to provide meaningful propulsive actuation in an LAO [2]. An LAO system makes use of the interaction between the Earth's geomagnetic field and an electrostatic charge built up on a satellite. Thus, LAO is a form of electromagnetic propulsion that does not require a tether. A tether system normally entails a long conductive wire through which a current is forced. The drifting electrons in the tether provide the moving charged particles necessary for the Lorentz force [3]. In LAOs, the spacecraft itself

becomes the moving charged particle, creating a current along its orbital path.

An LAO is achieved by a spacecraft that uses electrical power to build up a net electrostatic charge on its body, and this net charge causes an interaction between the geomagnetic field and the vehicle in the form of the Lorentz force. The magnitude and direction of the force are defined by the size and polarity of the charge on the satellite q , the velocity of the vehicle with respect to the magnetic field \mathbf{v}_r , and the strength and direction of the magnetic field \mathbf{B} :

$$\mathbf{F}_L = q(\mathbf{v} - \boldsymbol{\omega}_E \times \mathbf{r}) \times \mathbf{B} \quad (2)$$

where the position of the satellite is given by \mathbf{r} , and $\boldsymbol{\omega}_E$ represents the target planet's angular velocity. In an inertial frame, the geomagnetic field rotates with the planet [4]. This is true for other planetary magnetospheres as well. The relative velocity, \mathbf{v}_r , that defines the Lorentz force is the difference between the absolute spacecraft velocity, \mathbf{v} , and the velocity of the magnetic field, $\boldsymbol{\omega}_E \times \mathbf{r}$. A power system on the satellite can then modulate the net charge to control the propulsive force.

The LAO concept offers propellantless propulsion. The energy stored in a planet's rotation does work on the vehicle, creating an external force on the body without the expulsion of propellant. The size of the force is limited only by the charge-holding capacity (i.e., its self-capacitance) and the power constraints of the satellite. However, the direction of thrust is fixed with respect to the velocity direction of the spacecraft and the direction of the magnetic field. This direction limitation is not so restrictive as to render the system useless, though. Previously, we described methods for creating new Earth-synchronous orbits in low Earth orbit [5]. This paper addresses the use of LAO as a way to increase the flexibility and effectiveness of gravity-assist maneuvers. The methods used to analyze LAOs consist mainly of perturbations to Keplerian orbits, following our earlier work [5]. Section II provides an overview of relevant previous work with a primer on magnetospheres of the solar system and flyby trajectories, followed by a study of the extension of flybys that includes LAO dynamics. Adding the Lorentz force to hyperbolic trajectories creates several novel applications, including the arbitrary exit angle from the planet frame, propellantless capture, and flexible flyby timing.

II. Previous Work and Background Material

A. Previous Work

Lorentz force orbital perturbations have been observed in natural planetary systems [6–8]. Micron-sized dust grains are generally the most noticeably effected. These grains can acquire a large enough charge from their environment to have their orbits significantly changed. This phenomenon has been used to explain several subtleties in planetary ring systems.

In this study, we look at how actively controlling the charge on a spacecraft can be used to effect changes in its orbit. Previously, we

Presented as Paper 6846 at the AIAA Guidance, Navigation, and Controls Conference, Hilton Head, SC, 20–23 August 2007; received 14 November 2007; revision received 26 May 2009; accepted for publication 27 May 2009. Copyright © 2009 by Brett Streetman. Published by the American Institute of Aeronautics and Astronautics, Inc., with permission. Copies of this paper may be made for personal or internal use, on condition that the copier pay the \$10.00 per-copy fee to the Copyright Clearance Center, Inc., 222 Rosewood Drive, Danvers, MA 01923; include the code 0731-5090/09 and \$10.00 in correspondence with the CCC.

*Graduate Research Assistant, Department of Mechanical and Aerospace Engineering, 245 Upson Hall; currently Senior Member of the Technical Staff, Draper Laboratory, 555 Technology Square, Cambridge, MA 02139. Student Member AIAA.

†Assistant Professor, Department of Mechanical and Aerospace Engineering, 212 Upson Hall. Member AIAA.

derived perturbation equations for a satellite orbiting under the Lorentz force [5]. For any orbit, under the influence of any magnetic field, \mathbf{B} , the orbital energy of a spacecraft changes as

$$\dot{E} = (q/m)\omega_E[(\mathbf{v} \cdot \hat{\mathbf{n}})(\mathbf{B} \cdot \mathbf{r}) - (\mathbf{v} \cdot \mathbf{r})(\hat{\mathbf{n}} \cdot \mathbf{B})] \quad (3)$$

where \mathbf{r} is the position vector of the satellite, $\hat{\mathbf{n}}$ is a unit vector in the direction of the angular velocity of the central body, and ω_E is the magnitude of that angular velocity. The satellite's energy changes only due to the rotation of the central planet. The time rate of change of the spacecraft's angular momentum vector is

$$\dot{\mathbf{h}} = (q/m)(\mathbf{B} \cdot \mathbf{r})\mathbf{v} - (q/m)(\mathbf{r} \cdot \mathbf{v})\mathbf{B} - (q/m)\omega_E(\mathbf{B} \cdot \mathbf{r})(\hat{\mathbf{n}} \times \mathbf{r}) \quad (4)$$

The angular momentum of the satellite can change under the influence of a nonrotating magnetic field.

The combination of energy change and angular momentum change does not complete a full set of independent derivatives describing changes in the orbit. To more fully describe changes in the orbit, we use the eccentricity vector, \mathbf{e} . The eccentricity vector is defined as

$$\mathbf{e} = (\mathbf{v} \times \mathbf{h})/\mu - \hat{\mathbf{r}} \quad (5)$$

where $\hat{\mathbf{r}}$ is a unit vector in the radial direction. Physically, the eccentricity vector points from the center of the central planet toward the periapsis of the orbit. The magnitude of \mathbf{e} is equal to the orbital eccentricity, e . The time rate of change of \mathbf{e} due to the Lorentz force is

$$\dot{\mathbf{e}} = -(q/m)(1/\mu)\omega_E(\mathbf{B} \cdot \hat{\mathbf{n}})(\mathbf{r} \cdot \mathbf{v})\mathbf{r} + (q/m)(1/\mu)[\omega_E(\mathbf{B} \cdot \hat{\mathbf{n}})r^2 - (\mathbf{r} \times \mathbf{v}) \cdot \mathbf{B}]\mathbf{v} - (q/m)(1/\mu)(\mathbf{r} \cdot \mathbf{v})(\mathbf{v} \times \mathbf{B}) \quad (6)$$

Equations (3), (4), and (6) provide the information necessary to determine changes in five of the six orbital elements. Change in the semimajor axis, a , is calculated using the change in energy. Changes to the orbital inclination, i , and the right ascension of the ascending node, Ω , are found based on changes in the direction of the angular momentum vector. Changes in the eccentricity, e , and the longitude of periapsis, Π , can be gleaned from the change in the magnitude and direction of the eccentricity vector, respectively. The time rate of change of the true anomaly is derived independently in Sec. III.B.

B. Planetary Magnetic Fields

The LAO system requires an ambient magnetic field to work. The stronger a planet's magnetic field is, the more effective LAO can be. Russell provides a survey of planetary magnetospheres throughout the solar system [9]. Of the planets, six have appreciable internally generated magnetic fields (Mercury, Earth, Jupiter, Saturn, Uranus, and Neptune). Mars and Venus have such small and irregular fields that LAO is not a viable technique. Mercury's small magnetic (about 1/3000th of Earth's) and gravitational fields make it another unlikely LAO flyby target. The gas giants all have significant magnetic fields. Jupiter possesses by far the strongest magnetic field in the solar system, with a magnetic moment about 18,000 times as strong as Earth's. Table 1 lists the relative magnetic field strengths of each planet in the solar system.

The six planets with intrinsic magnetic fields all have relatively strong dipole components. This paper models all magnetic fields as dipoles with the dipole axis aligned with the planet's rotation axis. However, in most planets, the dipole component of the field is tilted at some angle. These angles are shown in Table 1. For the small tilt angles of Earth, Jupiter, and Saturn, equatorial orbits are relatively well modeled with a nontilted field [5]. The large tilt-angle fields of Neptune and Uranus are not considered here.

The impact of a significant tilt is that the energy of the orbit slowly drifts from its initial value [5]. A similar effect is evident in the angular momentum. The result is variability in inclination and eccentricity. Equations (3) and (4) account for these effects. The out-of-plane behaviors may prove valuable to some specific mission by accommodating plane-change requirements. Considering only the

Table 1 Comparison of planetary magnetospheres throughout the solar system

Planet	Orbit radius, AU	Magnetic moment [9] (compared with Earth)	Tilt of dipole component, deg [10]
Mercury	0.39	4×10^{-4}	14
Venus	0.72	~ 0	N/A
Earth	1	1	11.7
Mars	1.52	~ 0	N/A
Jupiter	5.20	1.8×10^4	9.6
Saturn	9.54	580	0.0
Uranus	19.2	50	58.6
Neptune	30.1	24	46.8

planar motion in this study limits the subsequent discussion to the ΔV and timing issues.

Jupiter and Earth are the most attractive targets for Lorentz augmentation of flyby maneuvers. Both planets are regularly used for gravity assists for interplanetary missions. This paper focuses on Jupiter flybys, but the analysis is valid for Earth and Saturn as well. Although Saturn is not convenient for gravitational flybys, its environment is well suited to LAO. The small tilt of its dipole component allows for a simpler and more effective controller to be implemented [5]. And, whereas Jupiter has a plasmasphere constantly being filled with charge-eroding ions from volcanic Io, Saturn has a much more benign radiation environment with no risk of LAO spacecraft interactions with heavily volcanic moons and a constant absorption of charged particles by the massive ring system.

The feasibility of achieving charge on a spacecraft has been the subject of previous works. Several architectures for charged spacecraft have been proposed [11], some of them based on recent, fundamental research on the physics of high-potential space structures [12]. Atchison and Peck have sized such a spacecraft for an outer-planet mission and find that a charge-to-mass ratio of 0.03 C/kg is within reach for known technologies [13].

C. Gravity-Assist Maneuvers

The gravity assist or flyby is a powerful tool in facilitating interplanetary missions. A gravity-assist maneuver uses the gravity well of a planet to alter the heliocentric orbit of a spacecraft. Interplanetary satellites have made extensive use of flybys since the Mariner 10 mission first used a flyby of Venus on its way to Mercury. In the simplest (but still quite accurate) analysis of a flyby maneuver, the hyperbolic trajectory of the spacecraft about the target planet is assumed to take a small amount of time compared with the planet's heliocentric orbit. This study also assumes all coplanar orbits and circular planetary paths. The sphere of influence approximation is also used. Schaub and Junkins [14] offer a more in-depth treatment of flybys and spheres of influence.

A gravity-assist maneuver uses the gravitational attraction of a target planet to rotate a portion of the heliocentric spacecraft velocity. In a heliocentric frame, the planet has a velocity of \mathbf{V}_p and the spacecraft has an initial heliocentric velocity of \mathbf{V}_{h1} . In a frame moving with the planet, the spacecraft has a velocity with respect to the planet of $\mathbf{v}_{in} = \mathbf{V}_{h1} - \mathbf{V}_p$ with a magnitude of v_∞ . Figure 1 depicts these quantities. The velocity, \mathbf{v}_{in} , and a periapsis distance, r_p , fix the planetocentric hyperbolic orbit. The periapsis distance is a free variable to be set by mission design. The eccentricity of this orbit gives the turning angle of the hyperbola, δ , through the relation $\sin(\delta/2) = 1/e$. The outbound planetocentric velocity of the spacecraft, \mathbf{v}_{out} , is equal in magnitude to the inbound velocity, \mathbf{v}_{in} , turned through the angle δ and having the same magnitude, v_∞ . The final heliocentric spacecraft velocity is then $\mathbf{V}_{h2} = \mathbf{v}_{out} + \mathbf{V}_p$. Thus, the spacecraft sees a heliocentric change in velocity of

$$\Delta V = 2v_\infty \sin(\delta/2) \quad (7)$$

The main goal of this study is to use the Lorentz force to rotate \mathbf{v}_{out} through an arbitrary angle γ , giving the mission designer much more freedom in obtaining a desired ΔV .

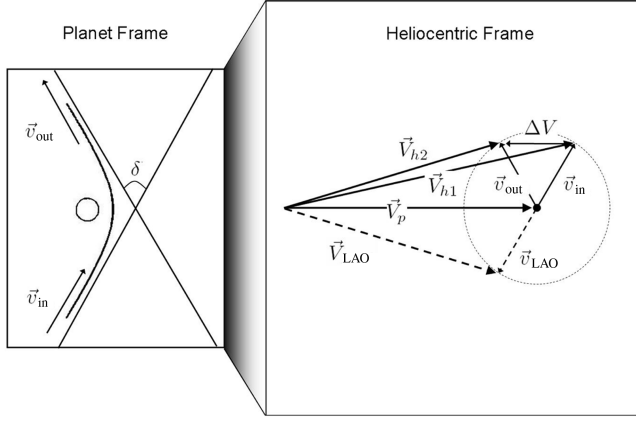


Fig. 1 Flyby trajectory vector definitions. The dotted vectors in the heliocentric view indicate a possible LAO trajectory resulting in a significantly larger ΔV .

Flybys can also be used to create multibody periodic orbits, such as the Aldrin cycler [15]. In the Aldrin orbit, repeated flybys of Earth and Mars are used to create a trajectory that cycles between the two planets, using much less fuel than single-use spacecraft making the same number of rendezvous. The Lorentz force can be used to make small adjustments to these types of Lorentz-augmented flyby maneuvers, further reducing the amount of fuel used by a cycler.

A final quantity of interest is the time of flight in the planetary frame. A mission plan requires an accurate assessment of the maneuver's duration. Time of flight in a hyperbolic orbit can be found from the hyperbolic anomaly, F . In terms of the true anomaly, ν , the hyperbolic anomaly is

$$F = \cosh^{-1} \left(\frac{e + \cos \nu}{1 + e \cos \nu} \right) \quad (8)$$

The hyperbolic anomaly can be related the mean anomaly, M , by

$$M = e \sinh F - F \quad (9)$$

Like Kepler's equation for eccentric anomaly, Eq. (9) cannot be solved in closed form. However, in certain special cases, the time of flight between two points in the orbit can be calculated. One such case is the time to travel between two symmetric points in the orbit (i.e., two points the same angular distance from periapsis). In this case, the resulting time of flight, Δt , is

$$\Delta t = 1/n(2e \sinh F - 2F) \quad (10)$$

where n is the mean motion of the satellite, and F is taken to be the positive of the two symmetric hyperbolic anomalies. For a hyperbolic orbit, n is defined as $\sqrt{\mu/(-a)^3}$, because the semimajor axis of a hyperbolic orbit is negative.

III. Applications

This section discusses two types of Lorentz-augmented flyby: changes during a single hyperbolic pass, and longer-duration maneuvers that involve a temporary capture at Jupiter. Both analytical and numerical techniques are used to study the costs and benefits of LAO maneuvers.

A. Single-Orbit Lorentz Modifications

On a single hyperbolic pass, the Lorentz force can change the orbit in several ways. For a constant charge applied throughout the orbit, both the semimajor axis and eccentricity of the orbit undergo transient changes but exhibit no net change over the course of the orbit. However, Π , the longitude of periapsis, undergoes a secular change throughout the orbit. Because only equatorial orbits are considered in this study, the longitude of periapsis, Π , is used to locate perijove rather than the more traditional argument of

periapsis, ω . Their difference is simple: the longitude of periapsis is measured from an inertially fixed x axis, whereas the argument of periapsis is measured from the line of nodes, which is undefined in an equatorial orbit. This change in the location of periapsis affects the asymptotic direction of the outbound leg of the hyperbola (without changing the magnitude of its velocity) and thus affects the outbound heliocentric velocity. If the charge on the satellite is modulated during the course of the orbit, the semimajor axis, eccentricity, and periapsis location can all be changed, affecting both the magnitude and direction of the outbound velocity.

We derive perturbation equations based on an osculating-element assumption. The perturbation equations are based on the general derivatives in Eqs. (3), (4), and (6), following the methods of Burns [16] and our earlier work [5]. The magnetic field of Jupiter is modeled as an axis-aligned dipole. A dipole model for the Jovian field is accurate enough for our purposes in a region from approximately 5–40 Jovian radii [13]. The Jovian dipole component is not axis aligned, but the tilt provides relatively small perturbations to orbits restricted to the equatorial plane. Here the small in-plane components of the magnetic field are ignored. We give an in-depth discussion of the effects of a tilted dipole model in our previous work [5].

We use the following vector model of a dipole field:

$$\mathbf{B} = (B_0/r^3)[3(\hat{\mathbf{N}} \cdot \hat{\mathbf{r}})\hat{\mathbf{r}} - \hat{\mathbf{N}}] \quad (11)$$

where $\hat{\mathbf{N}}$ is a unit vector along the magnetic north pole, and B_0 is the strength of the Jovian dipole field. Equation (11) is used along with standard Keplerian dynamics in Eq. (3). Relating changes in semimajor axis to changes in energy by taking the derivative of $E = -\mu/(2a)$ gives an expression for changes in semimajor axis due to the Lorentz force:

$$\dot{a} = 2 \frac{q}{m} B_0 \frac{\omega_E}{\sqrt{\mu}} \frac{a^2 e}{[a(1-e^2)]^{5/2}} \sin \nu (1 + e \cos \nu)^2 \quad (12)$$

Equation (6) is used to develop two further perturbation equations. The change in orbital eccentricity is

$$\dot{e} = \frac{q}{m} B_0 \left[\frac{\omega_E}{\sqrt{\mu}} - \frac{1-e^2}{[a(1-e^2)]^{3/2}} \right] \frac{\sin \nu}{[a(1-e^2)]^{3/2}} (1 + e \cos \nu)^2 \quad (13)$$

Directional changes in the eccentricity vector within the plane of the orbit directly correspond to changes in the location of periapsis. Solving for this angular change gives the time rate of change of longitude of periapsis as

$$\dot{\Pi} = \frac{q}{m} B_0 \left[\left(\frac{e^2 + 1}{[a(1-e^2)]^{3/2}} - \frac{\omega_E}{\sqrt{\mu}} \right) \cos \nu + \frac{2e}{[a(1-e^2)]^{3/2}} \right] \frac{(1 + e \cos \nu)^2}{e[a(1-e^2)]^{3/2}} \quad (14)$$

Whereas Eqs. (12) and (13) are periodic over true anomaly ν , Eq. (14) has a term that increases in a secular way. For a constant charge over several orbits, the semimajor axis and eccentricity repeat periodically, whereas the longitude of periapsis changes monotonically.

We use an osculating-element assumption to derive an expression for the average change in longitude of periapsis per orbit under the influence of a constant charge. The time rate of change of true anomaly is assumed to have its Keplerian value of

$$\dot{\nu} = \frac{\sqrt{\mu}(1 + e \cos \nu)^2}{[a(1-e^2)]^{3/2}} \quad (15)$$

Substituting this relationship into Eq. (14), integrating through one orbit, and solving for q/m gives

$$\frac{q}{m} = \Delta \Pi \frac{\sqrt{\mu}}{B_0} e \left[2 \left(\frac{e^2 + 1}{[a(1 - e^2)]^{3/2}} - \frac{\omega_E}{\sqrt{\mu}} \right) \sin v_\infty + \frac{4e}{[a(1 - e^2)]^{3/2}} v_\infty \right]^{-1} \quad (16)$$

where v_∞ is the true anomaly at infinity, given by $\cos v_\infty = -1/e$ for a hyperbolic orbit. Equation (16) is used to predict the charge-to-mass ratio required to obtain a particular change in the orbit.

Figure 2 shows the result of using Eq. (16) to model a rotation of an orbit. This simulation uses a two-body approximation with Jupiter as the sole source of gravity. All simulations in this study use two-body gravity with initial conditions that place the spacecraft at the edge of Jupiter's sphere of influence (SOI). The radius of Jupiter's SOI is [14]

$$R_{\text{SOI}} = (M_J/M_S)^{2/5} R_{S-J} \quad (17)$$

where M_J and M_S represent the masses of Jupiter and the sun, respectively, and R_{S-J} is the average distance between the two. By this definition, Jupiter's sphere of influence is about 48×10^6 km in radius. Although the SOI concept is not strictly correct, it is used here to facilitate a straightforward discussion of the orbital dynamics. Each simulation begins with the spacecraft on a Hohmann transfer orbit between Earth and Jupiter. At Jupiter, the spacecraft's velocity is parallel to the planet's. The Jupiter-centric orbit is fully defined by specifying a radius of perijove.

For the simulation displayed in Fig. 2, the perijove of the initial Keplerian hyperbola is 4 Jovian radii. This orbit (with $q/m = 0$ C/kg) is shown as solid black line in the figure. Equation (16) is then used to calculate the charge-to-mass ratio that results in a rotation of the hyperbolic exit asymptote of -30° . The resulting q/m is about -5.6 C/kg. The path of this spacecraft is shown as a dashed line in the figure.

Also shown in Fig. 2 is the path of a satellite with a q/m of -7.46 C/kg, represented by the dot-dash line. This value of the charge-to-mass ratio is calculated numerically to give exactly the requested -30° rotation. A simple numerical scheme is used for this calculation. An initial guess of q/m is obtained from Eq. (16). This value is used in a full numerical integration of the coupled perturbation equations, instead of the osculating approximation that led to Eq. (16). A simple Newton-Raphson solver is then employed over repeated integrations to find the value of q/m that accurately gives the desired orbit rotation.

Figure 2 clearly shows that results obtained using Eq. (16) are inaccurate. This solution gives an error of about 6° over a rotation of only 30° . As the size of the rotation increases, both the charge required and the perturbation error increase. One source of this error is the nature of a hyperbolic orbit. For most of the orbit, a satellite is

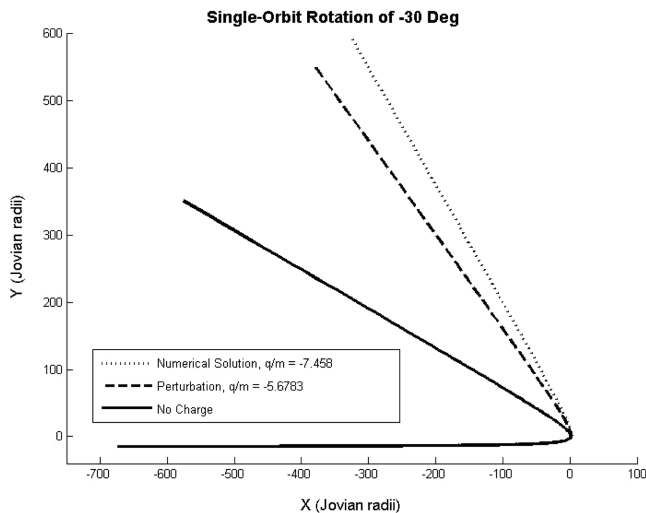


Fig. 2 Hyperbolic orbit for single-orbit rotation of periapsis, showing the Keplerian orbit, the numerically calculated solution, and the perturbation solution for the charge-to-mass ratio.

far from the central body and moving relatively slowly. However, around perijove, the satellite is close to the planet and moves extremely fast, making the Lorentz force much larger. This effect is demonstrated in Fig. 2. The inbound leg of each orbit shown is nearly identical. Only near perijove do the effects of the Lorentz force become apparent. The orbits of the LAO satellites undergo large changes in a short amount of time, undermining the accuracy of perturbation and osculating-element assumptions.

Small changes are easy to effect in a single hyperbolic pass. However, as the desired change to an orbit grows, the necessary charge required becomes prohibitively large. If a large enough change in exit angle is desired, the q/m necessary causes the osculating orbit assumption to break down in the presence of non-Keplerian orbit dynamics. Large changes are more easily and accurately brought about by slowly, repeatedly tweaking the orbit after temporarily capturing the satellite, as shown in the following sections.

One additional degree of freedom can be exploited in the single-pass modification: the charge-to-mass ratio does not need to be constant. With a variable charge-to-mass ratio the orbital energy, eccentricity, and exit angle can all be controlled to some extent. This type of maneuver is not expressly studied here, but, in the case of pure rotation, the charge required to make significant orbit changes becomes prohibitively large.

B. Lorentz-Augmented Capture

A readily apparent application of LAO is the capture of a spacecraft at a target planet. Atchison and Peck provide a detailed look at Lorentz-augmented capture at Jupiter [13]. They discuss the possibility of capturing satellites from many different entry orbits with charge-to-mass ratios as low as 0.005 C/kg. These captures are effected using a simple bang-bang charge controller. The capture maneuver is allowed to take up to 5 years over a large number of Jovian orbits. Atchison uses a conservative definition of capture that forces the satellite into a near-circular orbit at a reasonable distance from Jupiter.

This paper takes a slightly different approach to capture, as our main goal is to shape gravity-assist maneuvers, not facilitate planetary capture. Gravity assist involves hyperbolic orbits, for which the so-called excess velocity relates to the V that can be achieved. In the case of Atchison and Peck's study, the reduction of energy thanks to Lorentz force interactions was permitted to occur during many orbits. Therefore, we derive here expressions related to capturing a spacecraft in a single Jovian orbit. With a single-orbit capture, a satellite can temporarily stay in the neighborhood of Jupiter, allowing for adjustments in the timing and exit conditions of a flyby maneuver. Any spacecraft captured in a single orbit can also escape in a single orbit, with a charge of the same magnitude.

The quantity p , often called the orbit parameter or semilatus rectum, can be used to simplify the LAO analysis. The semilatus rectum is fundamentally connected to the magnitude of the angular momentum of the orbit, as in

$$p = h^2/\mu = a(1 - e^2) \quad (18)$$

In the same way as changes in the semimajor axis represent only changes in the orbital energy, changes in p reflect only changes in the angular momentum. Taking the derivative of Eq. (18) with respect to time yields

$$\dot{p} = \dot{a}(1 - e^2) - 2ae\dot{e} \quad (19)$$

Adapting this definition to an LAO by using Eqs. (12) and (13) gives

$$\dot{p} = 2(q/m)B_0(e/p^2) \sin v(1 + e \cos v)^2 \quad (20)$$

Equation (20), along with

$$\dot{e} = \frac{q}{m} B_0 \left[\frac{\omega_E}{\sqrt{\mu}} - \frac{1 - e^2}{p^{3/2}} \right] \sin v \frac{(1 + e \cos v)^2}{p^{3/2}} \quad (21)$$

$$\dot{\Pi} = \frac{q}{m} B_0 \left[\frac{1}{e} \left(\frac{e^2 + 1}{p^{3/2}} - \frac{\omega_E}{\sqrt{\mu}} \right) \cos v + \frac{2}{p^{3/2}} \right] \frac{(1 + e \cos v)^2}{p^{3/2}} \quad (22)$$

represents a new set of relevant LAO perturbation equations cast in terms of true anomaly, eccentricity, and semilatus rectum.

Adding to this set of perturbation equations is the Keplerian rate of change of true anomaly, recast with respect to p :

$$\dot{v} = \frac{\sqrt{\mu}(1 + e \cos v)^2}{p^{3/2}} \quad (23)$$

Equation (23) is substituted into the expression for the time rate of change of orbit parameter given in Eq. (20), with the following result:

$$p^{1/2} \dot{p} = 2(q/m)(B_0/\sqrt{\mu})e \sin v \dot{v} \quad (24)$$

Following the aforementioned procedure of integrating the perturbation equations about an orbit gives an integral of

$$\int_{p_0}^{p_1} p^{1/2} dp = 2 \frac{q}{m} \frac{B_0}{\sqrt{\mu}} e \int_0^\pi \sin v dv \quad (25)$$

The limits of integration for true anomaly are $v = 0$ to π . These limits correspond to a spacecraft that enters the Jovian SOI with no charge and remains free of charge until it reaches perijove. Once at perijove, the satellite turns on its charging mechanism. From perijove onward, a negative charge on the satellite decreases p . The semilatus rectum decreases until the orbit passes through unity eccentricity and becomes elliptical. We look only at cases in which the charge-to-mass ratio is sufficient to create an ellipse in one half-orbit. The spacecraft is captured in only half an orbit, and the problem is symmetric with respect to the line of nodes. These facts allow the capture to be reversed in only half an orbit as well. If the charge is on from apojove of the captured orbit until perijove, the parameter and eccentricity return to exactly the same values as the initial Jovian hyperbolic orbit.

Figures 3 and 4 demonstrate these principles through simulation. Figure 3 shows the capture of a satellite by LAO. Figure 3a shows the

spacecraft's trajectory through Jovian space. The satellite is initially on the Earth–Jupiter Hohmann ellipse, with a perijove of 1.05 Jovian radii. Figure 3b displays both the true anomaly of the satellite and its charge-to-mass ratio on one set of axes. The charge is initially zero on the hyperbolic entry and is then changed to -1.098 C/kg as the satellite passes through perijove. This charge causes energy to be removed from the satellite's orbit. The charge then remains constant through the resulting elliptical orbit. The trajectory plot also clearly shows the rotation of the longitude of periapsis caused by the constant charge. Figure 4 shows the eventual escape of the same spacecraft. The charge is initially at the negative value of -1.098 C/kg. Then, as the satellite passes perijove, the charge is set to zero, allowing the vehicle to resume its initial hyperbolic orbit (albeit rotated through some angle).

Solving the integral in Eq. (25) gives a relationship between a charge applied from perijove to apojove and the final semilatus rectum:

$$\frac{q}{m} = \frac{1}{6} \frac{(p_1^{3/2} - p_0^{3/2})\sqrt{\mu}}{B_0 e_0} \quad (26)$$

where p_0 is the parameter of the initial hyperbolic orbit, and p_1 represents the final elliptical orbit. Unlike the semimajor axis, p varies smoothly through the transition between hyperbolic, parabolic, and elliptical orbits.

Using the parameter p instead of the semimajor axis simplifies many of the perturbation equations. However, the semimajor axis is often the quantity of most interest in capture problems. Defining a not only sets the size of the orbit, but also its period. Knowing the period of the captured orbit becomes important as we attempt to shape a flyby.

We can find how the energy (and, thus, the semimajor axis) change as p changes. Whereas a particular parameter p can correspond to many different values of the semimajor axis and eccentricity, the Lorentz force only changes the quantities in a specific, related way. The particular nature of the Lorentz force causes the spacecraft to follow only certain trajectories in the state-space plane defined by p

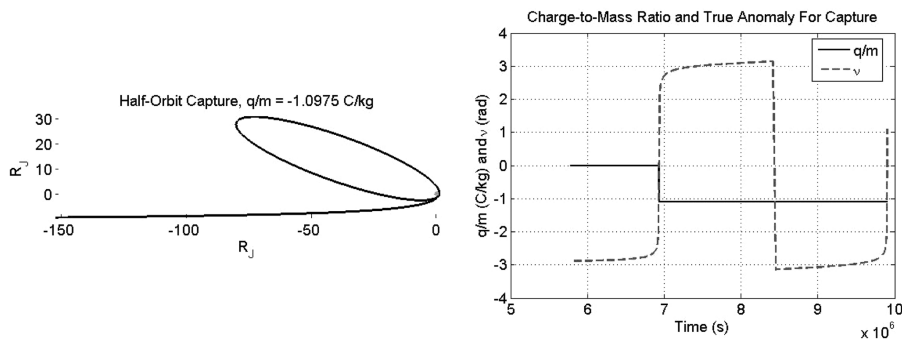


Fig. 3 Capture of an LAO spacecraft in one half-orbit: a) orbital track of the satellite, and b) true anomaly of the spacecraft and the charge on it. The charge is turned on as the spacecraft passes through perijove and remains on as it is captured.

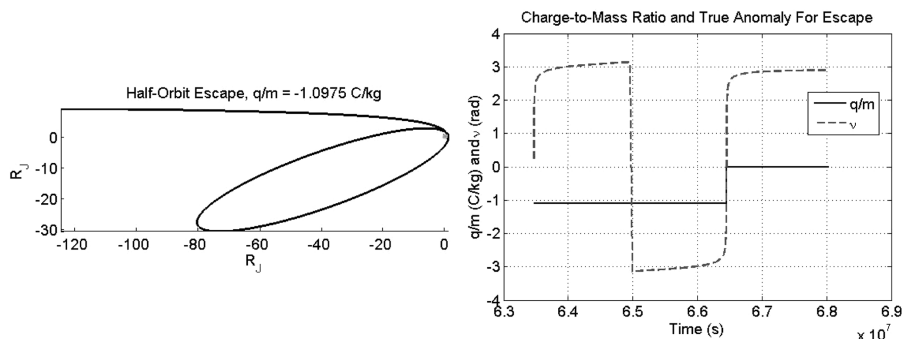


Fig. 4 Escape of an LAO spacecraft in one half-orbit: a) orbital track of the satellite, and b) true anomaly of the spacecraft and the charge on it. The charge is initially on and is then turned off as the spacecraft passes through perijove.

and E . We use our perturbation equations to solve for these p - E trajectories based on the satellite's initial orbit. First, recall the LAO perturbation to energy, recast in terms of p :

$$\dot{E} = (q/m)\omega_E B_0(e/p) \sin v \dot{v} \quad (27)$$

Recognizing and equating the similar terms in Eq. (27) and the derivative of p given in Eq. (20) gives an equation relating changes in semilatus rectum to changes in orbital energy:

$$\dot{p} = (2/\omega_E \sqrt{\mu}) p^{1/2} \dot{E} \quad (28)$$

Equation (28) defines a certain trajectory in the p - E space; it is a separable differential equation and can be solved. Energy is used rather than semimajor axis because, like p , E varies smoothly across the hyperbolic-elliptical transition. Separating and integrating gives

$$p_1 = [(1/\omega_E \sqrt{\mu})(E_1 - E_0) + p_0^{1/2}]^2 \quad (29)$$

where E_0 and E_1 refer to the initial hyperbolic and final elliptical orbits, respectively. Semimajor axis can now be substituted for orbital energy, giving

$$p_1 = \{(-\sqrt{\mu}/2\omega_E)[(1/a_1) - (1/a_0)] + p_0^{1/2}\}^2 \quad (30)$$

where the 0 and 1 subscripts are as above. Equation (30) now allows us to specify a final semimajor axis, a_1 , for the captured orbit. Specifying a_1 in turn defines the final desired semilatus rectum p_1 . This parameter value is then used in Eq. (26), which gives a q/m that results in the desired final orbit size.

C. Flyby Shaping Using a Temporary Jovian Capture

Two methods are examined for augmenting a gravity-assist maneuver with a temporary capture at Jupiter. In the first case, a captured satellite simply waits in a stable parking orbit for a specified time period. During the wait, the orbital motion of Jupiter causes the exit heliocentric of the spacecraft to be different than otherwise possible. The second method involves active specification of the outbound orbit. The spacecraft is captured and then uses a constant charge to change its perijove location. This perijove rotation enables an arbitrary exit direction from the planet and much more flexibility in designing the heliocentric Δv achieved by the satellite.

The simplest application of a temporary LAO capture at Jupiter is a timing maneuver. A spacecraft enters the Jovian SOI on a hyperbolic trajectory and is captured by turning on its charge-building mechanism at perijove, as described earlier. As the satellite reaches the apojuve of its new elliptical orbit, the excess charge is removed. The spacecraft is in a stable elliptical orbit. With zero net charge on the satellite, this elliptical orbit remains unchanged.

The goal of such a capture is to create more favorable timing for a flyby maneuver. This wait at Jupiter can extend or create new launch windows or create a more favorable geometry for reaching potential targets. A satellite can leave Earth when Jupiter is in a favorable position for rendezvous and then hold at Jupiter until the best time for leaving Jupiter for the eventual target. This method could potentially open many new mission windows as, instead of waiting for a relatively rare alignment of Earth-Jupiter-target, the spacecraft can be launched at any Earth-Jupiter alignment (which occurs every 1.093 years) [14]. When the mission calls for the spacecraft to leave the vicinity of Jupiter, a charge of the same magnitude as the capture maneuver is turned on at apojuve of the ellipse. By perijove, the satellite has regained energy such that it is in its original hyperbolic orbit. The charge is turned off and the spacecraft escapes. The maneuver can be timed easily by choosing an elliptical orbit for which the period is an integer divisor of the desired waiting time.

In addition to merely timing a flyby, a temporary capture at Jupiter can provide greater freedom in designing a gravity assist. Instead of waiting in a static ellipse during the timing maneuver, LAO is used to evolve the ellipse. By correctly choosing the magnitude of a constant charge, an arbitrary exit angle from Jupiter's SOI is achieved. Obtaining an arbitrary exit allows for the full range of ΔV

possibilities of the flyby to be used. In Fig. 1, the dotted lines show a possible LAO trajectory for which the maximum magnitude of ΔV is obtained. The change in velocity can range anywhere from $\Delta V = 0$ to $2v_\infty$.

One way to accomplish an arbitrary exit angle is to use a large enough charge that the spacecraft goes from the hyperbolic entrance trajectory all the way to a circular orbit. This effect is achieved "instantaneously" at perijove of the hyperbola. As the satellite is an equatorial orbit, moving purely tangentially to Jupiter, the Lorentz force on it is purely radial in direction. This radial force can cancel or augment the gravitational force such that the satellite continues to move in a circular orbit until the charge is turned off. Once the charge is turned off, the satellite resumes its previous hyperbolic orbit, escaping the system. Peck [2] gives a more in-depth discussion of this type of maneuver.

Although the straight-to-circle maneuver is simple, the magnitude of charge-to-mass ratios it requires are infeasible. A method requiring less charge to complete the same maneuver is a temporary capture into an elliptical orbit, followed by successive changes in longitude of perijove. As perijove rotates, the exit asymptote of the escape hyperbola rotates as well. A careful choice of the capture ellipse properties allows a constant charge to be found that both captures the satellite and rotates the exit angle through a desired value in an integer number of orbits. This process is depicted in Fig. 5, which shows the four stages of the capture and precess scenario. First, the spacecraft enters the Jovian SOI on a hyperbolic trajectory with zero charge until perijove. Second, the increased charge causes the capture of the satellite into a closed orbit. Third, the constant charge on the satellite causes the captured orbit to precess. Note that this orbit is not a Keplerian ellipse. The Lorentz force is constantly acting on the spacecraft, changing its trajectory. These changes are only substantial near perijove. Fourth, the charge is removed at a subsequent perijove, enable the spacecraft to escape once again.

To solve for this required charge-to-mass ratio, we define an angle γ as the angle between the incoming asymptote of the hyperbola and the desired outgoing asymptote. Thus, a value of $\gamma = 2\pi$ represents an outgoing hyperbolic leg that is exactly antiparallel to the incoming orbit. This value of γ maximizes the magnitude of the ΔV for the flyby maneuver. An angle of $\gamma = \pi$ represents the minimum magnitude of ΔV , with the satellite exiting along a path exactly parallel to its inbound trajectory, causing the overall change in velocity to be zero.

With a given γ , it is not possible in general to specify the exact amount of time in which the arbitrary exit angle maneuver happens. Forcing both a constant charge and an integer number of orbits for the rotation places too many constraints on the problem. In the solution presented here, a maximum time for the maneuver to happen, t_{\max} , is

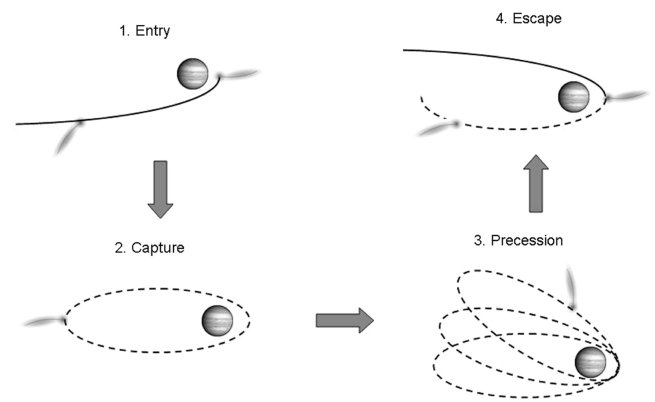


Fig. 5 The four stages of the capture and precess scenario. First, the spacecraft enters the Jovian SOI on a hyperbolic trajectory with zero charge until perijove. Second, the increased charge causes the capture of the satellite into a closed orbit. Third, the constant charge on the satellite causes the captured orbit to precess. Fourth, the charge is removed at a subsequent perijove, enabling the spacecraft to escape once again. Dotted lines indicate times when the charge is nonzero, and solid lines indicate zero charge.

specified and then the solution closest to that amount of time is solved for. In general, the longer the maneuver, the higher the number of orbits, N , and the lower the charge-to-mass ratio required. To find the best solution, a initial guess of N is used to find a solution that is iterated to find the largest permissible N .

To complete a rotation through γ in N orbits, an average change in longitude of periapsis of

$$\dot{\Pi}_{\text{avg}} = \frac{\gamma - (\pi - \delta)}{N \cdot 2\pi \sqrt{a_1^3/\mu}} \quad (31)$$

is required, where a_1 is the semimajor axis of the capture ellipse. This periapsis change rate is used in

$$\frac{q}{m} = \frac{\dot{\Pi}_{\text{des}} a_1^{3/2} p^{3/2}}{2B_0} \quad (32)$$

which is the perturbation solution charge-to-mass ratio required for an average rate of change of periapsis through an elliptical orbit. However, a_1 is currently unknown, but we can equate the expressions for the charge-to-mass ratio for both capture and rotation as

$$(q/m)_{\Delta\Pi} = (q/m)_{\Delta p} \quad (33)$$

where $(q/m)_{\Delta\Pi}$ is taken from Eq. (32), and $(q/m)_{\Delta p}$ is from Eq. (26). Combining these two expressions and using Eq. (30) gives

$$\begin{aligned} &(\dot{\Pi}_{\text{des}} a_1^{3/2} - (\sqrt{\mu}/3e_0))\{(-\sqrt{\mu}/2\omega_E)[(1/a_1) - (1/a_0)] + p_0^{1/2}\}^3 \\ &+ (\sqrt{\mu}/3e_0)p_0^{3/2} = 0 \end{aligned} \quad (34)$$

where $\dot{\Pi}_{\text{des}}$ is given in Eq. (31). For a given γ and N , Eq. (34) gives the perturbation solution to the temporary capture with an arbitrary rotation problem. Solving this equation for a_1 gives the size of the capture ellipse, which sets the q/m required. The specified charge is turned on at perijove of the initial hyperbola. The spacecraft is then captured to an ellipse. As the constant charge remains on, the elliptical orbit rotates. After exactly N orbits, the charge is removed, allowing the spacecraft to reenter its initial hyperbolic orbit. However, this orbit has been rotated such that the exit asymptote of the hyperbola is an angle γ away from the inbound half of the orbit.

An algorithm for the solving the maximum time problem presented here is as follows:

- 1) Define the maximum maneuver time t_{max} .
- 2) Define the outgoing angle γ .
- 3) Set $N = 1$.
- 4) Solve Eq. (34) to find a_1 and, thus, the required q/m .
- 5) Return to step 3 and increment N until $N \cdot 2\pi \sqrt{a_1^3/\mu} > t_{\text{max}}$.

This algorithm represents the perturbation solution for this problem. But, as discussed earlier, perturbation methods have several inaccuracies that are especially apparent under hyperbolic LAOs. In the case of the temporary capture, arbitrary exit problem, these perturbation errors compound through both inaccurate capture and inaccurate rotation expressions that propagate through several orbits, leading to large errors over the course of the maneuver. These errors make the perturbation solution impractical. Thus, we develop a numerical solution that uses the perturbation solution as an initial guess.

A numerical solution of the arbitrary exit problem requires a set of equations for the change in orbital elements due to the Lorentz force. Although Eqs. (20–22) are quite accurate, the assumptions made to analytically manipulate them introduce errors. These three equations can be numerically integrated with respect to true anomaly for an accurate depiction of an LAO. However, the Lorentz force causes changes in the true anomaly, ν . These changes are especially important in hyperbolic or high-eccentricity elliptical orbits. In these orbits, the true anomaly changes slowly away from periapsis and then rapidly near periapsis. In these periods of rapid changes, small errors in the assumed Keplerian time rate of change of true anomaly result in large errors in the actual angle. Here we derive a perturbation expression for the rate of true anomaly change. This expression, when combined with the set of other perturbation solutions, creates a

much more accurate system describing the effects of the Lorentz forces on a satellite.

An expression for true anomaly is obtained from the standard equation for the radius of a conic section orbit:

$$\cos \nu = (1/e)[(p/r) - 1] \quad (35)$$

In the absence of all perturbative forces, the derivative of Eq. (35) yields the standard derivative of true anomaly given in Eq. (15), where p and e are constants, and \dot{r} is known from conservation of angular momentum. Once the perturbation force is taken into account, \dot{p} and \dot{e} are no longer zero, and the derivative of Eq. (35) is

$$\sin \nu \dot{\nu} = (p/er^2)\dot{r} - (\dot{p}/er) + (1/e^2)[(p/r) - 1]\dot{e} \quad (36)$$

Equation (36) is valid for any perturbation, not solely the Lorentz force. For an LAO specifically, \dot{p} and \dot{e} are replaced by Eqs. (20) and (21), respectively. For an instantaneous application of the Lorentz force, \dot{r} does not change from its Keplerian value. Combining these expressions gives the time rate of change of true anomaly for a charged spacecraft:

$$\begin{aligned} \dot{\nu} = &\left[\sqrt{\mu} - 2 \frac{q}{m} B_0 \frac{(1 + e \cos \nu)}{p^{3/2}} \right. \\ &\left. + \frac{q}{m} B_0 \left(\frac{\omega_E}{\sqrt{\mu}} - \frac{1 - e^2}{p^{3/2}} \right) \frac{\cos \nu}{e} \right] \frac{(1 + e \cos \nu)^2}{p^{3/2}} \end{aligned} \quad (37)$$

The first term in brackets represents the Keplerian secular increase in ν . The second and third terms represent the fact that the true anomaly changes when semilatus rectum and orbital eccentricity change.

With Eqs. (20–22), Eq. (37) completes a full set of accurate differential equations for the temporary capture problem. (As the problem is restricted to the equatorial plane, inclination and right ascension can be ignored.) With this set of equations, a numerical algorithm is developed to solve the problem. This algorithm is mainly an extension of the aforementioned perturbation method and is as follows:

- 1) Define the maximum maneuver time t_{max} .
- 2) Define the outgoing angle γ .
- 3) Set $N = 1$.
- 4) Solve Eq. (34) to find an initial guess for a_1 .
- 5) Solve (by repeated numerical integrations) for the q/m that gives exactly a_1 (at apojove) for the captured ellipse.
- 6) Check (numerically) what rate of longitude of periapsis change this q/m gives. If this rate is not equal to the desired rate, go to step 4 and adjust the guess for a_1 until $\dot{\Pi}_{\text{actual}} - \dot{\Pi}_{\text{des}} = 0$.
- 7) Return to step 3 and increment N until $N \cdot 2\pi \sqrt{a_1^3/\mu} > t_{\text{max}}$.

This algorithm solves the arbitrary exit angle by temporary capture problem quite accurately. Figure 6 shows an orbital trajectory solved for using this algorithm, with $\gamma = 2\pi$ and $N = 20$. This simulation uses all the same initial conditions as those mentioned earlier. The spacecraft enters Jupiter's sphere of influence on a Hohmann trajectory from Earth with a perijove of 1.05 Jovian radii. The charge on the satellite is zero until the it reaches perijove of the initial hyperbolic orbit. The spacecraft's charge is then brought up to -1.098 C/kg and held constant. This charge captures the satellite and then rotates the resulting ellipse through 20 full orbits. After exactly 20 orbits, the charge is removed, allowing the spacecraft to return to a hyperbola, exiting the Jovian SOI in exactly the opposite direction as its entrance. This time history of charge-to-mass ratio is shown in Fig. 7.

Figure 8 shows the orbital eccentricity of the spacecraft throughout the maneuver. This figure reveals the nature of the captured orbit. Shown on the figure is a dotted line representing an eccentricity of 1, which separates elliptical from hyperbolic orbits. Initially, the spacecraft is in a hyperbolic orbit, with an eccentricity greater than 1. When the charge is turned on, e begins dropping sharply. Before the spacecraft can leave the Jovian SOI, the eccentricity drops below 1, showing that the satellite is now in a captured, elliptical orbit. As the spacecraft passes through apojove, e begins to increase again until, at

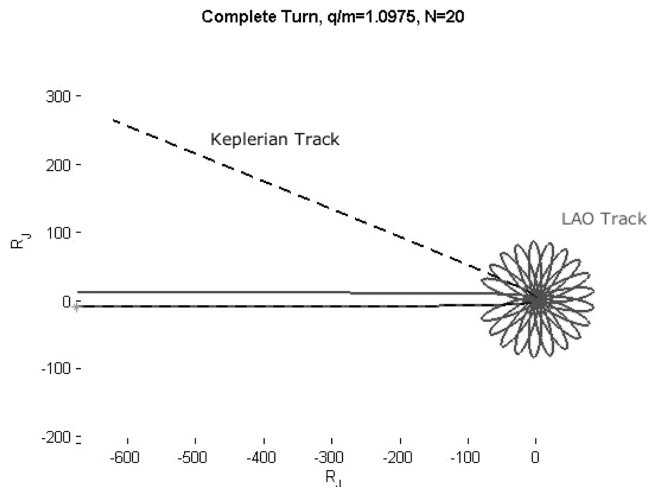


Fig. 6 Arbitrary exit flyby trajectory. The chosen exit angle is 2π , or exactly opposite of the entrance angle. The number of elliptical orbits is 20, and the charge-to-mass ratio is -1.098 C/kg.

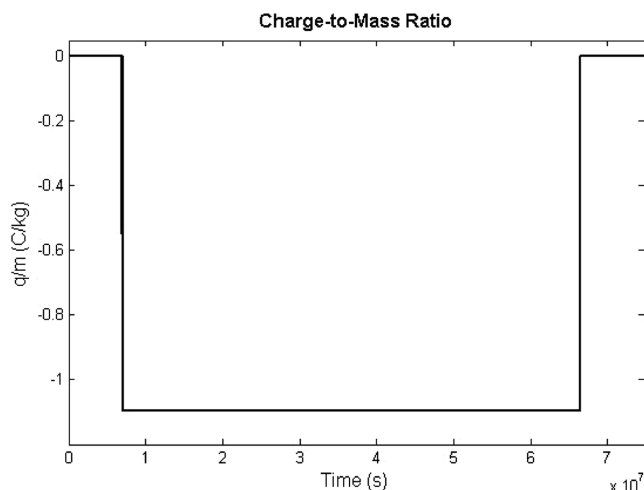


Fig. 7 Arbitrary exit flyby charge-to-mass ratio. q/m is initially 0 and then increases to -1.098 C/kg at the first perijove. The charge remains constant through all 20 orbits and goes to 0 at the final perijove.

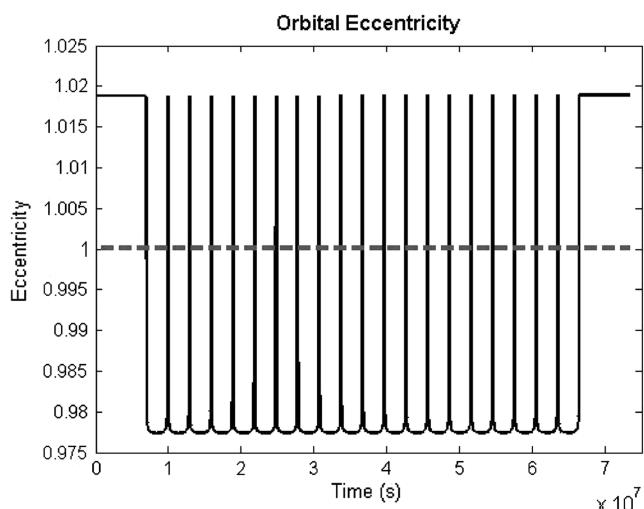


Fig. 8 Arbitrary exit flyby orbital eccentricity. The eccentricity is initially hyperbolic, but is reduced to an elliptical value. Through each orbit, e oscillates between values above and below 1, until the final escape.

perijove, it has reached its initial hyperbolic value. In an osculating sense, the satellite is in a hyperbolic orbit at perijove, but, as long as the charge remains on, the spacecraft continues on a non-Keplerian, but closed orbit. After the prescribed number of orbits, the charge is returned to zero. The osculating orbit becomes the true orbit, and the satellite escapes.

This simulation depicts about 849 days. The initial hyperbolic orbit with no temporary capture would last 321 days from the entrance of Jupiter's SOI to exit. Thus, the maneuver itself adds 528 days to the Jovian flyby. In essence, time is traded for a more effective flyby using a smaller charge. Although the single-pass method adds no time to the flyby, it uses a q/m of -7.5 C/kg to rotate the orbit 30 deg. The temporary capture adds 528 days, but can rotate the orbit through a full 360 deg for only -1.01 C/kg. Generally, the smallest q/m values that allow for temporary capture are on the order of -1 C/kg (with maneuver time increasing greatly for small decreases in charge). Although the temporary capture method can add significant time to a flyby maneuver, this time may actually be beneficial to the mission, allowing for extended launch windows and additional science opportunities. This method is a powerful way to add flexibility and effectiveness to a flyby using a simple on-off charge on the satellite. More advanced charge modulation could extend the method even further.

III. Conclusions

The LAO is shown to have valuable and significant effects on gravity-assist maneuvers without the expenditure of propellant. Either with a single pass or with a temporary capture at a the flyby target, LAO can greatly change the exit characteristics and timing of a flyby. The effective ΔV of a gravity assist can be maximized (or minimized). Temporary capture allows for the duration of a maneuver to be arbitrarily extended, opening up longer and more flexible mission windows. These effects are derived analytically to provide insight, although perturbation solutions prove to be quantitatively inaccurate. Numerical integrations are used to confirm the applications found with analytical solutions.

References

- [1] D'Amario, L., Byrnes, D., and Stanford, R., "Interplanetary Trajectory Optimization with Application to Galileo," *Journal of Guidance, Control, and Dynamics*, Vol. 5, No. 5, 1982, pp. 465–471. doi:10.2514/3.56194
- [2] Peck, M. A., "Prospects and Challenges for Lorentz-Augmented Orbits," AIAA Paper 2005-5995, Aug. 2005.
- [3] Cosmo, M. L., and Lorenzini, E. C., *Tethers in Space Handbook*, 3rd ed., NASA Marshall Space Flight Center, Huntsville, AL, 1997.
- [4] Rothwell, P. L., "The Superposition of Rotating and Stationary Magnetic Sources: Implications for the Auroral Region," *Physics of Plasmas*, Vol. 10, No. 7, 2003, pp. 2971–2977. doi:10.1063/1.1582473
- [5] Streetman, B., and Peck, M. A., "New Synchronous Orbits Using the Geomagnetic Lorentz Force," *Journal of Guidance, Control, and Dynamics*, Vol. 30, No. 6, 2007, pp. 1677–1690. doi:10.2514/1.29080; also AIAA Paper 0731-5090.
- [6] Schaffer, L., and Burns, J. A., "The Dynamics of Weakly Charged Dust: Motion Through Jupiter's Gravitational and Magnetic Fields," *Journal of Geophysical Research*, Vol. 92, 1987, pp. 2264–2280. doi:10.1029/JA092iA03p02264
- [7] Schaffer, L., and Burns, J. A., "Charged Dust in Planetary Magnetospheres: Hamiltonian Dynamics and Numerical Simulations for Highly Charged Grains," *Journal of Geophysical Research*, Vol. 99, 1994, pp. 17211–17223. doi:10.1029/94JA01231
- [8] Hamilton, D. P., "Motion of Dust in a Planetary Magnetosphere: Orbit-Averaged Equations for Oblateness, Electromagnetic, and Radiation Forces with Applications to Saturn's F Ring," *Icarus*, Vol. 101, 1993, pp. 244–264; Erratum: *Icarus*, Vol. 103, p. 161. doi:10.1006/icar.1993.1022
- [9] Russell, C. T., "Planetary Magnetospheres," *Reports on Progress in Physics*, Vol. 56, 1993, pp. 687–732. doi:10.1088/0034-4885/56/6/001
- [10] Ness, N. F., "Intrinsic Magnetic Fields of the Planets: Mercury to Neptune," *Philosophical Transactions of the Royal Society of London*.

- Series A, Physical Sciences and Engineering*, Vol. 349, No. 1690, 1994, pp. 249–260.
doi:10.1098/rsta.1994.0129
- [11] Hoyt, R., and Minor, B., “Remediation of Radiation Belts Using Electrostatic Tether Structures,” *Proceedings of the IEEE Aerospace Conference*, Inst. of Electrical and Electronics Engineers, Los Alamitos, CA, March 2005, pp. 583–594.
- [12] Choinière, E., and Gilchrist, B. E., “Self-Consistent 2-D Kinetic Simulations of High-Voltage Plasma Sheaths Surrounding Ion-Attracting Conductive Cylinders in Flowing Plasmas,” *IEEE Transactions on Plasma Science*, Vol. 35, No. 1, 2007, pp. 7–22.
doi:10.1109/TPS.2006.889300
- [13] Atchison, J., and Peck, M., “Lorentz Augmentation in Jovian Captures,” *Journal of Guidance, Control, and Dynamics*, Vol. 32, No. 2, 2009, pp. 418–423.
doi:10.2514/1.38406
- [14] Schaub, H., and Junkins, J. L., *Analytical Mechanics of Space Systems*, AIAA, Reston, VA, 2003.
- [15] Byrnes, D. V., Longuski, J. M., and Aldrin, B., “Cycler Orbit Between Earth and Mars,” *Journal of Spacecraft and Rockets*, Vol. 30, No. 3, 1993, pp. 334–336.
doi:10.2514/3.25519
- [16] Burns, J. A., “Elementary Derivation of the Perturbation Equations of Celestial Mechanics,” *American Journal of Physics*, Vol. 44, No. 10, 1976, pp. 944–949.
doi:10.1119/1.10237